

The Modeling of Dough Mixing with Free Surfaces in Two and Three dimensions

M.F. Webster, D. Ding & K.S. Sujatha

*Institute of Non-Newtonian Fluid Mechanics, University of Wales Swansea
SA2 8PP, UK.*

Abstract

This paper reports work on the two and three-dimensional numerical simulation of dough mixing with free surfaces, that arises in the food processing industry. Free surface flow in a rotating cylinder is investigated when a fluid is mixed in a cylinder with a stirrer. Different dough mixer designs are investigated. The rotating stirrer may be placed either in a concentric or eccentric arrangement with respect to the axis of the vessel being horizontal or vertical. The equations are solved in a three dimensional cylindrical polar coordinate system. The numerical simulation is based on a Taylor-Galerkin finite element formation, with an arbitrary Lagrangian-Eulerian scheme to accommodate free surface movement. Predictions compare closely to equivalent experimental results.

1 Introduction

This paper addresses the two and three-dimensional numerical simulation of dough mixing with free surfaces, that arises in the food processing industry. The motivation for this work is to develop an advanced technology to model dough mixing. The ultimate objective is to provide a predictive capability from which optimal designs for dough mixers may emerge. Two different dough mixer designs are investigated. The single rotating stirrer is placed either in a concentric or eccentric arrangement, with respect to the axis of the vessel in the first and second instance. As an alternative to the conventional mixer, the motion is assumed to be driven by the rotation of the vessel in the present work.

The mixer is considered in a vertical (r, θ, z) and horizontal (r, θ) orientation and to be partially-filled during the process. This leaves the surface of the fluid to move freely. Special considerations are applied to the free surface, that is described by a number of particles. The movement of each particle is traced by an explicit

Eulerian scheme. Peeling and wetting conditions between the fluid and solid surfaces are investigated. In a horizontal orientation, peeling may be observed at the contact point between the advancing surface and the solid boundary, whilst wetting may be observed at the contact point between the dragging surface and the solid wall of the vessel. In the case of vertical orientation with the outer vessel moving, wetting occurs at the outer vessel and peeling at the inner stirrer. The stretch (or strain-rate) of a segment of the free surface is used as a criterion to monitor peeling and wetting. Stretch is monitored via the ratio of the newly calculated length of the segment against its initial length. Peeling or wetting is detected if a free surface segment contacting the solid boundary is stretched/contracted beyond some limiting criteria. When this occurs, the free surface is retarded by relaxing the newly calculated position. The velocity of the free surface is adjusted accordingly, to relieve the level of stressing.

The simulation employs a Taylor-Galerkin finite element formation for the generalised Navier-Stokes equations. The formation applies a temporal discretisation in a Taylor series, prior to a Galerkin spatial discretisation. A semi-implicit treatment for diffusion is used to address linear stability constraints. The flow is modeled as incompressible via a pressure-correction procedure. An arbitrary Lagrangian-Eulerian scheme is adopted to accommodate free surface movement. A fixed finite element mesh covers the whole domain, that is divided dynamically into two different sections: one wet and another dry. The position of the free surface defines the fluid region. The solution of the field variables is activated only within the wet fluid zone. Inelastic materials are considered in the present work, though this will be extended to consider viscoelastic fluid models.

2 Basic equations and numerical scheme

A Carreau-Yasuda model, represented by equation 1 below, is employed to describe the shear-thinning behaviour of the viscosity μ ,

$$\mu = \frac{\mu_0 - \mu_\infty}{1 + (\lambda\dot{\gamma})^m} + \mu_\infty \quad (1)$$

where μ_0 is a reference viscosity at low shear rates and μ_∞ is an asymptotic value of viscosity at large shear rates; $\dot{\gamma} = 0.5\sqrt{I_2}$ with the second invariant I_2 of the rate-of-strain tensor, m is a powerlaw index and λ is a material constant.

For the convenience, the following non-dimensionalisation is adopted

$$x^* = \frac{x}{L}, \quad u^* = \frac{u}{V}, \quad \mu^* = \frac{\mu}{\mu_c}, \quad (2)$$

where L , V and μ_c are characteristic length, velocity and viscosity respectively. We take L to be the diameter of the stirrer, V to be the speed of the vessel, μ_c to be $\mu_0 (= 1.05 \text{ Pa}\cdot\text{s})$. This leads to a Reynolds number, the only non-dimensional group number involved, defined as

$$Re = \frac{\rho LV}{\mu_c} \quad (3)$$

where ρ is the fluid density. Hereforth, we discard the * notation for ease of presentation. To be specific we take $m = 0.6$ and $\lambda = 0.083s$.

The algorithm invoked in this work follows references 1-3. Briefly, a Taylor-Galerkin algorithm is employed to solve the governing equations relating to the conservation of mass and momentum. A time stepping scheme is derived through Taylor series expansions up to second order in time step and a two-step predictor-corrector scheme is assumed. This, in conjunction with a second-order pressure correction method to accommodate the incompressibility constraint, produces a fractional-staged equation system to solve of three distinct phases over each time step. A semi-implicit treatment of a Crank-Nicolson type is adopted for diffusion terms. A Galerkin finite element spatial discretisation renders a fully discrete system with the choice of piecewise continuous quadratics for velocity, and linears for pressure. The system is specified as

stage 1a:

$$\left[\frac{2Re}{\Delta t} M + \frac{1}{2} S_u \right] (U^{n+\frac{1}{2}} - U^n) = \{-[S_u U + Re N(U)U] + L^T P\}^n \quad (4)$$

stage 1b:

$$\left[\frac{Re}{\Delta t} M + \frac{1}{2} S_u \right] (U^* - U^n) = [-S_u U + L^T P]^n - Re[N(U)U]^{n+\frac{1}{2}} \quad (5)$$

stage 2:

$$K(P^{n+1} - P^n) = -\frac{2}{\Delta t} LU^* \quad (6)$$

stage 3:

$$\frac{Re}{\Delta t} M(U^{n+1} - U^*) = \frac{1}{2} L^T (P^{n+1} - P^n) \quad (7)$$

where U^n , U^{n+1} , P^n and P^{n+1} are nodal vectors of velocity and pressure at time t^n and t^{n+1} respectively; U^* is an intermediate nodal velocity vector introduced in step 1b; M , S_u , $N(U)$, K and L are mass matrix, momentum diffusion matrix, convection matrix, pressure stiffness matrix and divergence-pressure gradient matrix, respectively. The details of the above matrices can be found in the background literature, ref [1-3].

3 Free surface tracking

An arbitrary Lagrangian-Eulerian method is employed to deal with free surfaces. A fixed finite element mesh applies to the flow domain that is divided dynamically into two distinct parts: one wet and another dry. The position of the free surface defines the fluid region and the domain of solution. The solution of the field variables, such as velocity, pressure and stress, are instigated within only the wet

fluid zone.

3.1 Particle tracking scheme

Free surface profiles are obtained by tracking particle histories. It is assumed that the fluid surface consists of particles. For tracking the position, a well-established explicit Euler scheme is adopted,

$$x_p^{n+1} = x_p^n + \Delta t v(x_p, t^n) \quad (8)$$

where, for particle p , x_p^n is a position at time t^n , $v(x_p, t^n)$ is a velocity at x_p^n at time t^n , x_p^{n+1} is a position at time t^{n+1} . This scheme is performed after stage 3 of each time step of the Taylor-Galerkin algorithm, i.e., at the end of each time-step cycle. For practical convenience, a small gap is introduced between the first particle and the cylinder wall to avoid dealing with fixed particles under no-slip.

At the end of each time step, the most up to date wet and dry regions are identified and the status of all nodes noted accordingly, as to whether wet or dry. In the finite element calculation, the wet and dry regions are distinguished by appropriate material properties assigned to each quadrature point.

3.2 Peeling/wetting on free surfaces

Peeling or wetting is controlled by assessing the stretch ratio of a contacting point between the fluid and the solid boundary, which is directly proportional to the local stress experienced. Peeling or wetting is recognised to occur if a limiting stretch value (α) of a line surface segment nearest the solid boundary is exceeded,

$$\frac{\Delta l_i^{n+1}}{\Delta l_i^0} \geq \alpha. \quad (9)$$

Here, Δl_i^0 and Δl_i^{n+1} represent the length of a segment i adjacent to a solid boundary at time $t = 0$ and t^{n+1} respectively. For both horizontal and vertical orientation with one stirrer, the limiting value α is taken as 5 at the outer vessel and 2 at the inner stirrer. In the three-dimensional vertical orientation of the vessel, wetting is also controlled by the angle θ made between the wall and the line segment connecting the particle on the wall and the nearest neighbour particle on the same radial line. If this angle is less than, say 20° , the latter particle will be attached to the wall. The position of a free surface is then adjusted by relaxing the newly calculated position by a certain degree, say 50%.

4 Problem specification

For the three-dimensional simulation, a cylindrical vessel with a stirrer placed concentric to the axis of the vessel is considered. The fluid is driven by the outer wall and fixed at the top of the vessel by a lid as shown in Fig 1. Tetrahedral elements are employed. To create a three-dimensional finite element mesh, first

each brick element is formed, which is then divided into six tetrahedra. This leads to 6000 tetrahedral elements, 9240 velocity nodes and 1320 pressure nodes. At the start of the simulation, the vessel is 60% full. The outer vessel, attached to the bottom plate, rotates at different rotational speeds and the top is held stationary.

For the two-dimensional case, the flow geometry is discretised into a triangular mesh, with piecewise linear interpolation functions for pressure and quadratic interpolation functions for velocity. The geometry is shown in Fig 2. The flow domain is discretised into 240 triangular elements, 520 velocity nodes and 140 pressure nodes.

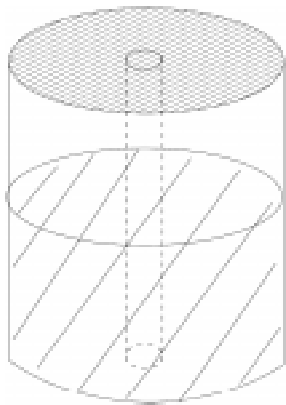


Figure 1. Vertical view(3D):
Vessel with one stirrer

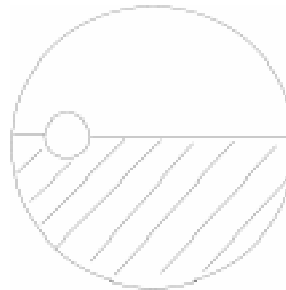


Figure 2. Horizontal view(2D):
Flow domain and moving surface

5 Results

Numerical simulations for the above mentioned problems have been conducted at various speeds. The results reflect close agreement against equivalent experimental results.

Free surface profiles are plotted at steady states for different speeds, namely, 100, 150 and 200 r.p.m, and compared with the equivalent experimental plots. Figure 3 demonstrates a typical comparison set. Figure 4 shows the development of the fluid free- surface in time against experimental results. Since the surface is symmetric, the geometry is sliced at the center along the axis and the surface positions are plotted in two dimensions.

The fluid motion starts from rest and the surface is in a horizontal orientation. As time progresses, the fluid wets the outer wall and peels away from the stirrer, due to the centrifugal force. The final steady position is noted to take up a parabolic shape.

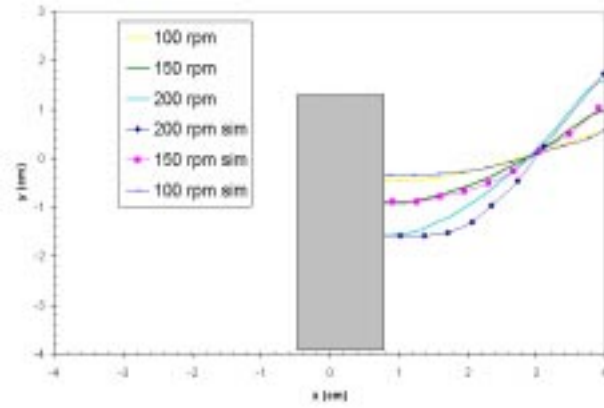


Figure 3. Surface positions with speeds, comparison against experiment

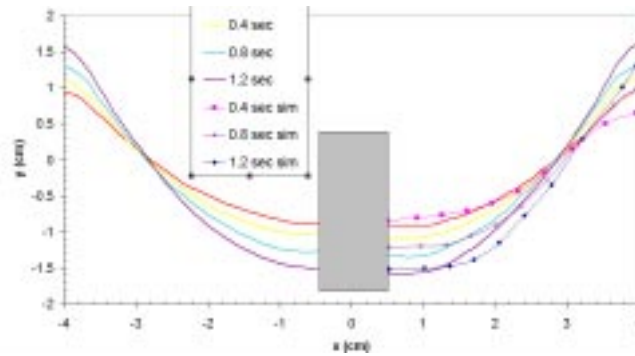


Figure 4. Surface positions with time, comparison against experiment

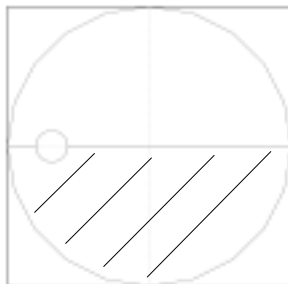


Figure 5. Surface position at start.

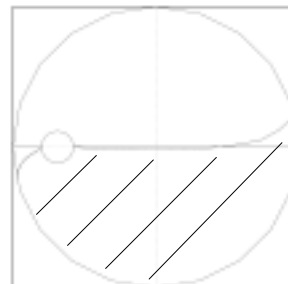


Figure 6. Surface position at a quarter of rotation.

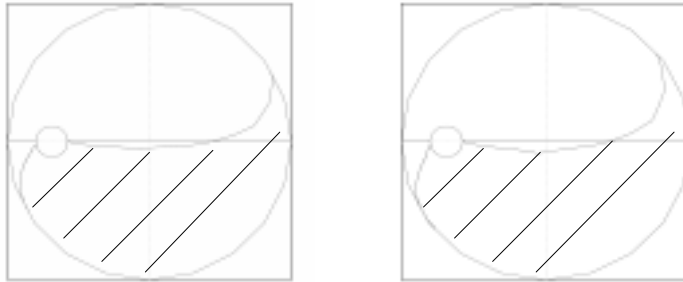


Figure 7. Surface position at 2 rotations. Figure 8. Surface position at 20 rotations.

Figures 5-8 show the deformation patterns of the free surfaces whilst the vessel rotates at the start, a quarter of a rotation, two rotations and after twenty rotations. It is observed that the free surfaces move smoothly and approach a steady state after some twenty rotations of the vessel. The peeling-and-wetting phenomena are observed at the contact point, between the dragging surface and the vessel, as shown in Figures 7 and 8. The effect of wetting is to push more segments of the surface onto the vessel. Peeling is also observed at the contact point, between the dragging surface and the stirrer, as shown in Figures 7 and 8. Peeling is not apparent at the forward-driving surface, because of the asymmetry of the geometry.

6 Conclusions

We have successfully demonstrated the use of a numerical flow solver for non-Newtonian fluids, along with an arbitrary Lagrangian–Eulerian scheme to track free-surfaces as a predicting tool for this industrial flow problems. We have been able to provide physically realistic simulations for this complex mixing process. We are presently addressing the transient free surface problem and the phenomena of wetting-and-peeling boundary contact, in more complex geometries. For example with two stirrers, and with vertical and horizontal orientations in three dimensions. This will take us closer to the actual mixing process.

7 Refences

- [1] D. M. Hawken, H. R. Tamaddon-Jahromi, P. Townsend, and M.F. Webster, A Taylor-Galerkin-based algorithm for viscous incompressible flow. *Int. J. Num. Meth. Fluids*, **10(3)**, pp. 327-351, 1990.
- [2] D. Ding, P. Townsend, and M. F. Webster, On computations of two and three-dimensional unsteady thermal non-Newtonian flows. *Int. J. Num. Meth. Heat Fluid Flow*, **5(6)**, pp. 495-510, 1995.
- [3] H. Matallah, P. Townsend, and M. F. Webster, Recovery and stress-splitting schemes for viscoelastic flows. *J. Non-Newtonian Fluid Mech.* **75**, pp. 139-166, 1998.
- [4] D. M. Binding, and M. Couch, personal communication, 2000.